



HAL
open science

Ideal Chern bands are Landau levels in curved space

Benoît Estienne, Nicolas Regnault, Valentin Crépel

► **To cite this version:**

Benoît Estienne, Nicolas Regnault, Valentin Crépel. Ideal Chern bands are Landau levels in curved space. *Physical Review Research*, 2023, 5 (3), pp.L032048. 10.1103/PhysRevResearch.5.L032048 . hal-04084064

HAL Id: hal-04084064

<https://hal.science/hal-04084064v1>

Submitted on 5 Oct 2023

HAL is a multi-disciplinary open access archive for the deposit and dissemination of scientific research documents, whether they are published or not. The documents may come from teaching and research institutions in France or abroad, or from public or private research centers.

L'archive ouverte pluridisciplinaire **HAL**, est destinée au dépôt et à la diffusion de documents scientifiques de niveau recherche, publiés ou non, émanant des établissements d'enseignement et de recherche français ou étrangers, des laboratoires publics ou privés.



Distributed under a Creative Commons Attribution 4.0 International License

Ideal Chern bands as Landau levels in curved space


Benoit Estienne¹, Nicolas Regnault^{2,3} and Valentin Crépel⁴

¹*Sorbonne Université, CNRS, Laboratoire de Physique Théorique et Hautes Énergies, LPTHE, F-75005 Paris, France*

²*Laboratoire de Physique de l'École Normale Supérieure, ENS, Université PSL, CNRS, Sorbonne Université, Université Paris-Diderot, Sorbonne Paris Cité, 75005 Paris, France*

³*Department of Physics, Columbia University, New York, New York 10027, USA*

⁴*Center for Computational Quantum Physics, Flatiron Institute, New York, New York 10010, USA*

 (Received 4 April 2023; revised 27 July 2023; accepted 11 September 2023; published 29 September 2023)

We prove that all the criteria proposed in the literature to identify a Chern band hosting exact fractional Chern insulating ground states, in fact, describe an equivalence with a lowest Landau level defined in curved space under a nonuniform magnetic field. In addition, we design an operational test for the most general instance of such lowest Landau-level mapping, which only relies on the computationally inexpensive evaluation of Bloch wavefunctions' derivatives. Our work clarifies the common origin of various Chern-idealness criteria, proves that these criteria exhaust all possible lowest Landau levels, and hints at classes of Chern bands that may possess interesting phases beyond Landau level physics.

DOI: [10.1103/PhysRevResearch.5.L032048](https://doi.org/10.1103/PhysRevResearch.5.L032048)

Introduction. The remarkable promise of fractional Chern insulators (FCIs) [1–4], is to realize the universal anyonic physics existing in fractional quantum Hall (FQH) systems [5–19] using less stringent experimental conditions, and in particular, without any external magnetic field. At the same time, FCIs remain fragile strongly correlated phases of matter, and abundant theoretical research efforts aimed at identifying propitious conditions for their emergence. Arguably, some of the most promising insights towards that goal originated from the realization that $|C| = 1$ Chern bands with constant quantum geometric tensor (QGT) reproduce the interaction form factors of the standard lowest Landau-level (LLL) wavefunctions on the torus [20]. As a result, the interacting physics of both systems are identical, allowing one to transpose most of our analytical understanding of FQH systems to such bands. This LLL-mapping argument identifies certain bands in which analytical arguments can ensure the emergence of FCIs, and can serve as a guide in our long-standing search for zero-field analogs of FQH states.

Motivated by recent progress in moiré systems [21–28], more general conditions have been obtained to capture a larger set of bands in which FCIs appear as the ground state of a specific interacting Hamiltonian at fractional filling. These various criteria for idealness have introduced a zoology of special Chern bands, those of constant QGT carrying the name “flat Kähler bands” [29–31], which were joined by “ideal bands” featuring a nonuniform QGT that nevertheless possesses a constant null vector [32], which were themselves extended to so-called “vortexable bands” allowing

for nonlinear embedding in real space [33]. Each of these classes is defined by the ability to obtain a model interacting Hamiltonian for FCIs, akin to the pseudopotentials in FQH systems [34].

This raises the question whether these apparently different classes of Chern bands have a common physical origin, and whether the number of classes will keep growing as new model Hamiltonians are found or will instead converge to a complete definition. In this work, we convey concrete answers about these two questions.

First, we prove that all currently existing criteria for special bands with unit Chern number are generalized versions of LLL mapping, accounting for a nonuniform magnetic field and cyclotron metric. The former enables one to describe the fluctuation of the QGT of ideal bands, while the latter captures how the density profile of Bloch states changes near their zeros at different points in space and encompasses the nonlinear embedding of “vortexable” bands. Second, we conversely demonstrate that the most general class of periodic LLL can be reproduced by at least one of the special Chern bands so far introduced, bolstering the generality of Ref. [33]. An ideal Chern band, in the most liberal sense, is therefore in one-to-one mapping with a LLL, proving that there cannot exist more general criteria describing Chern idealness by analogy with LLLs. Third, we extend the demonstration to higher Chern numbers using their color decomposition [35]. Finally, we design an operational criterion to test which Chern bands can be mapped a LLL with nonuniform magnetic field and metric. Our criterion only involves derivatives of the Bloch eigenfunctions, and therefore remains computationally inexpensive.

Most general periodic lowest Landau level. The Landau problem describes the quantization of cyclotron orbits of free massive charged particles in a magnetic field $B = \varepsilon^{ab} \partial_a A_b$ on a two-dimensional plane. In the simplest scenario where the mass tensor and magnetic field are uniform, the spectrum is

Published by the American Physical Society under the terms of the [Creative Commons Attribution 4.0 International](https://creativecommons.org/licenses/by/4.0/) license. Further distribution of this work must maintain attribution to the author(s) and the published article's title, journal citation, and DOI.

composed of Landau levels (LLs), which are equally spaced energy levels with extensive degeneracy due to the unconstrained guiding center degree of freedom. On allowing for a nonuniform mass tensor or a curved plane, a metric g_{ab} is introduced, but the spacing and degeneracy of LLs are not compromised as long as the magnetic flux density B/\sqrt{g} remains constant, where $\sqrt{g} = \sqrt{\det g_{ab}}$ [36–39]. In all other cases, LLs generically exhibit a finite dispersion. However, the LLL can still be flattened and locked at zero energy by adding an electric potential $V = B/(2\sqrt{g})$ [40]. Therefore, the most generic flat LLL on a plane can be obtained by considering the ground-state manifold $\mathcal{L}(g, B)$ of the Hamiltonian

$$\mathcal{H}(g, B) = \frac{1}{2\sqrt{g}}[\pi_a g^{ab} \sqrt{g} \pi_b - B], \quad (1)$$

with $\pi_a = -i\partial_a - A_a$ the canonical momentum (we use units in which the Planck's constant, the electric charge, and mass are equal to 1, $\hbar = e = m = 1$).

To capture the physics of periodic two-dimensional systems, we convert these LLLs into a band problem. For this to happen, the metric and the magnetic field must be periodic with respect to a Bravais lattice $\mathbb{Z}a_1 + \mathbb{Z}a_2$, with an integer number of flux quanta N_ϕ per unit cell. This last requirement ensures that the magnetic translations T_j by a_j for $j = 1, 2$ commute and can be simultaneously diagonalized. The number of bands obtained via this construction is equal to N_ϕ . Since we are interested in describing a single band, we fix $N_\phi = 1$ from now on.

To find the LLL of $\mathcal{H}(g, B)$, it is convenient to use isothermal coordinates (X, Y) in which the metric is $ds^2 = e^{2\sigma(X, Y)}(dX^2 + dY^2)$ with σ a real function [41]. The complex coordinate $Z = X + iY$ can be chosen such that $Z(r + a_1) = Z(r) + 1$ and $Z(r + a_2) = Z(r) + \tau$, where τ is a complex number, and $r = (x, y)$ denotes the original coordinate system [42]. The Hamiltonian becomes $\mathcal{H}(g, B) = \frac{1}{2m}e^{-2\sigma}\Pi\bar{\Pi}$ where $\Pi = \pi_X + i\pi_Y$, and LLL wavefunctions are those annihilated by $\bar{\Pi}$. This property is conformally invariant, it is not sensitive to the conformal factor $e^{2\sigma}$, and LLL wavefunctions are invariant, up to normalization, under Weyl transformation (local rescaling of the metric).

To be more explicit, we split the total magnetic field as $B = B_0 + \tilde{B}$ where $B_0 = 2\pi/\text{Im}\tau$ is uniform in isothermal coordinates and \tilde{B} carries no flux on the unit cell. The LLL wavefunction $|\psi_k\rangle \in \mathcal{L}(g, B)$ diagonalizing the magnetic translations $T_j|\psi_k\rangle = e^{ik_j}|\psi_k\rangle$ takes the first-quantized form [42]

$$\psi_k(x, y) = e^{-\tilde{\rho}(X, Y)}\phi_k(X, Y)/N_k, \quad (2)$$

where (i) $|\phi_k\rangle \in \mathcal{L}(\delta_{ab}, B_0)$ denotes the wavefunction of the LLL defined on the torus $\mathbb{C}/(\mathbb{Z} + \tau\mathbb{Z})$ with uniform and isotropic metric, and displaying the same magnetic translation eigenvalues as $|\psi_k\rangle$, (ii) $\tilde{\rho}$ stands for the periodic Poisson (or Kähler) potential representing the fluctuating part of the magnetic field, i.e., $\Delta\tilde{\rho} = \tilde{B}/\sqrt{g}$ in the original metric, and (iii) $N_k^2 = \int dX dY |e^{\sigma-\tilde{\rho}}\phi_k|^2$ is the normalization constant carrying information about the local space curvature. For completeness, we also provide the explicit form of flat and uniform LLL functions [42]

$$\phi_k(X, Y) = e^{(B_0/4)Z(Z-\bar{Z})+i(k_1+\pi)Z}\theta_1(Z - Z_k; \tau), \quad (3)$$

whose zero is fully determined by the quasimomentum that fixes $2\pi Z_k = (k_2 + \pi) - \tau(k_1 + \pi)$, where we have used the symmetric gauge and denoted as θ_1 the first Jacobi theta function.

To conclude, the most generic LLL $\mathcal{L}(g, B)$ can be written as that of the conformally equivalent flat surface using isothermal coordinates, with the addition of a periodic Poisson field and a scalar product that correctly includes the Jacobian of the transformation to the new coordinates.

Equivalence with ideal bands. In this Letter, our first goal is to show that any ideal Chern band (for all flavors of idealness introduced in the literature) maps to a LLL $\mathcal{L}(g, B)$ for some choice of nonuniform field and metric. Here, mapping means that the scalar product and form factors computed within the Chern band can be reproduced using LLL wavefunctions from Eq. (2), ensuring that both systems share the same interacting phase diagram. This definition allows the single-particle wavefunctions of both systems to solely differ by an overall spatially dependent phase factor, i.e., for all ψ_C in the ideal Chern band there exists ψ_L in $\mathcal{L}(g, B)$ such that $\psi_C = e^{is}\psi_L$ with s a real function independent of ψ_C . This phase factor is needed to reconcile the respective periodic and the quasiperiodic magnetic boundary conditions of ψ_C and ψ_L . Equivalence up to this boundary condition sewing phase factor shall be written $\psi_C \equiv \psi_L$ in the rest of this work.

We split the discussion into two parts, considering first the momentum-space condition for idealness involving the QGT [20,32], before turning to the real-space ‘‘vortexability’’ criterion [33]. We focus on the case $C = 1$, relegating the discussion of greater Chern number to the end of the Letter.

Momentum-space condition. Consider a $C = 1$ Chern band spanned by Bloch wavefunctions $|\psi_k\rangle$ of unit-cell periodic parts $|u_k\rangle = e^{-ik\cdot r}|\psi_k\rangle$, the quasimomentum k fixing the eigenvalues under the two elementary translations of the lattice $\psi_k(r + a_j) = e^{ik_j}\psi_k(r)$. Then, define the quantum geometric tensor as $\mathcal{Q}_k^{ab} = \langle D_k^a u_k | D_k^b u_k \rangle$ using the covariant derivative $D_k^a = \partial_k^a - \langle u_k | \partial_k^a | u_k \rangle$. The band is said to be q ideal if \mathcal{Q} possesses a constant null vector w throughout the Brillouin zone: $\mathcal{Q}_k^{ab}w_b = 0$ for all k .

The relation between q -ideal bands and LLs has already been acknowledged [32,43], and follows from two main observations. First, the null vector condition is equivalent to the momentum-space holomorphicity of the cell periodic Bloch vectors $Q(k)[w_a \partial_k^a |u_k\rangle] = 0$, where $Q(k) = 1 - |u_k\rangle\langle u_k|$ and $\partial_k^a = \partial/\partial k_a$ [44]. Second, this holomorphicity condition stringently constrains the $|\psi_k\rangle$ to admit a universal form descending from a Landau level $\psi_k(r) \equiv e^{-\tilde{\rho}(r)}\phi_k(r)/N_k$ [32], with $e^{-\tilde{\rho}(r)}$ a real positive and periodic function [45], and $|\phi_k\rangle \in \mathcal{L}(g_{ab} = \text{Re}[w_a w_b^*], B_0 = 2\pi/|a_1 \times a_2|)$ the element of a uniform LLL diagonalizing the magnetic translations by $a_{j=1,2}$ with eigenvalues e^{ik_j} . These magnetic translations commute due to the choice of B_0 , which corresponds to having a single flux quantum threading each unit cell in the Landau problem. Finally, the scalar product remains the canonical one on the plane, such that $N_k^2 = \int d^2r |e^{-\tilde{\rho}}\phi_k|^2$.

Written in this form, the q -ideal band considered can be straightforwardly mapped onto the generalized LLL of Eq. (2) using the linear transformation $Z = X + iY = w_a x^a$, which transforms the metric into $g_{ab}dx^a dx^b = dZ d\bar{Z}$ [we have performed a global rescaling and rotation to fix $Z(a_1) = 1$]. The

TABLE I. Summary of the two types of ideal bands, the type of $\mathcal{L}(g, B)$ they map onto (see text), and the corresponding currently known test of idealness.. For r -ideal bands, \mathcal{Q}^F denotes the quantum geometric tensor computed using the $|u_k^F\rangle$ ensuing from the nonlinear embedding of the unit cell F .

Type	g	B	Test
q ideal	Uniform	Any	$\int_{BZ} \det \mathcal{Q}_k = 0$ [32]
r ideal	Any	Any	$\min_F \int_{BZ} \det \mathcal{Q}_k^F = 0$ [33]

parameter τ of the torus is determined from the magnetic boundary conditions $\tau = Z(a_2)$ [32]. Finally, we observe that B_0 and $\tilde{\rho}$ are defined identically here and in Eq. (2), completing the mapping of q -ideal Chern bands to LLLs with isotropic and uniform metric but spatially varying magnetic fields $\mathcal{L}(\delta_{ab}, B_0 + \tilde{B})$, already hinted at in previous works [43,46,47].

Real-space condition. The momentum-space condition for idealness has been generalized to a larger family of Chern bands [33]. In more detail, a band \mathcal{C} is r ideal if there exists a function $\mathfrak{z} : \mathbb{R}^2 \mapsto \mathbb{C}$, which, for periodic systems, must satisfy $\mathfrak{z}(r + a_j) = \mathfrak{z}(r) + \mathfrak{z}(a_j)$, and if \mathcal{C} is stable under multiplication by \mathfrak{z} . Due to its transformation under lattice translations, \mathfrak{z} can be viewed as a nonlinear real-space unit cell embedding, or equivalently, as a change of coordinates $F : r \rightarrow \mathfrak{r}$. Here, the term ‘‘band’’ underlies translation symmetry on a lattice with generating vectors denoted by $a_{1,2}$, and we may choose $\mathfrak{z}(a_1) = 1$ and $\mathfrak{z}(a_2) = \tau$ as above.

Reference [33] observed a relation between r -ideal and q -ideal bands when using the F nonlinear embedding to modify the periodic part of the Bloch functions $|u_k\rangle = e^{-i(k,\mathfrak{r})} |\psi_k\rangle$, with $(k, \mathfrak{r}) = k_a M^{ab} \mathfrak{r}_b$ defined by the real invertible matrix M^{ab} solving the two equations $M^{ab} \mathfrak{r}_b(a_i) = a_i^a$. Then, the stability of \mathcal{C} under \mathfrak{z} multiplication becomes equivalent to the requirement of momentum-space holomorphicity for the $|u_k\rangle$ [33,42]. In particular, this implies that r idealness is more general than q idealness due to the allowed nonlinear embedding of the unit cell. Quoting the result for q -ideal bands, we infer that the Bloch wavefunctions of \mathcal{C} can be expressed as $\psi_k(r) \equiv e^{-\tilde{\rho}(\mathfrak{r})} \phi_k(\mathfrak{r})/N_k$. The only difference with q -ideal bands being the normalization factor $N_k^2 = \int d^2\mathfrak{r} |J_F| \cdot |e^{-\tilde{\rho}} \phi_k|^2$, which features the Jacobian J_F of F .

This is sufficient to map r -ideal bands to the LLL of Eq. (2). Isothermal coordinates are obtained as in the q -ideal case through $Z = X + iY = w_a \mathfrak{r}^a$, where we similarly have imposed $Z(a_1) = 1$ and defined $\tau = Z(a_2)$. To reproduce the normalization of r -ideal bands, we want the metric of the analog LLL to feature the same Jacobian factor $ds^2 = |J_F|(dX^2 + dY^2)$, which is accomplished using $g = |J_F(r)|g(r)$ with $g_{ab} = \text{Re}[\partial_a \mathfrak{z}^* \partial_b \mathfrak{z}]$. Once the metric is known, $\tilde{\rho}$ and \tilde{B} are obtained as in the q -ideal case. This concludes the mapping of r -ideal bands to the LLL $\mathcal{L}(g, B)$, where both g and B need to be periodic to capture the nonuniformity of the Berry curvature and the normalization of the more general r -ideal bands (see Table I for a summary).

Exhaustion of all periodic LLLs. We have just proved that any ideal bands can be mapped to the most general form of a Landau level $\mathcal{L}(g, B)$ with periodic metric and magnetic field

[Eq. (2)]. Conversely, any LLL $\mathcal{L}(g, B)$ is trivially an r -ideal band. Indeed, the $\mathcal{L}(g, B)$ are stable under multiplication by $Z = X + iY$, the complex isothermal coordinate, a property inherited from the flat and uniform LLLs spanned by the ϕ_k of Eq. (3). Hence, ideal bands are in one-to-one correspondence with LLL in curved space with nonuniform magnetic fields. Ideal bands do not exist beyond those already identified in the literature.

Indiscriminate LLL mapping criterion. We now turn to the practical problem of probing LLL mapping in its most general form. In Table I, we summarize the existing tests for checking whether a band is q or r ideal. The probe for the more restrictive q idealness is computationally inexpensive. It only necessitates the calculation of the quantum geometric tensor over the full Brillouin zone, that is, the evaluation of the momentum derivatives of the $|\psi_k\rangle$. On the other hand, no efficient test of r idealness exists at the moment. One could check the q -idealness condition with the quantum metric \mathcal{Q}^F defined with $|u_k^F\rangle = e^{-ik \cdot F(r)} |\psi_k\rangle$ for all possible changes of coordinates F . This should be understood as a consequence of the connection between r -ideal and q -ideal bands more than an actual probe because of the unpractical minimization over all nonlinear embeddings F .

By explicit construction, we show that an operational test discriminating bands that map to the most general periodic LLL, and only involves derivatives of the Bloch wavefunctions, is possible. We first rationalize our criterion using some general properties of $\mathcal{L}(g, B)$, and then check that it indeed provides a criterion for LLL equivalence when applied to Chern bands.

Starting from Eq. (2), and remembering that $\phi_k(X, Y)$ is a product of an analytical function in $Z = X + iY$ with a k -independent nonholomorphic form factor, we observe that

$$\lambda_k : r \rightarrow \psi_k(r)/\psi_0(r) \tag{4}$$

is meromorphic in Z ; the origin of the Brillouin zone $k = 0$ can be arbitrarily chosen. The complex structure corresponding to this meromorphicity can be obtained as

$$J_k = (d\lambda_k)^{-1} J d\lambda_k, \quad d\lambda_k = \begin{bmatrix} \partial_1 \text{Re } \lambda_k & \partial_2 \text{Re } \lambda_k \\ \partial_1 \text{Im } \lambda_k & \partial_2 \text{Im } \lambda_k \end{bmatrix}, \tag{5}$$

of the complex plane’s canonical $J_{ij} = \varepsilon_{ij}$. Note that the J_k and invariant under the gauge transformation $\psi_k \rightarrow e^{i\theta_k} \psi_k$. Because Z is momentum independent, so should the complex structure J_k be. This statement forms the operational probe of LLL mapping that we propose:

$$\partial_k^a J_k = 0. \tag{6}$$

A straightforward calculation [42] shows that Eq. (6) indeed holds for the ideal bands of Ref. [33].

Let us now prove that bands fulfilling Eq. (6) map onto a LLL $\mathcal{L}(g, B)$. In that case, each of the differentiable function λ_k defined by Eq. (4) is holomorphic with respect to the complex structure J_k defined by Eq. (5), except where its poles lie. For generic physical systems, ψ_0 only features isolated zeros that do not produce essential singularities. The λ_k are thus meromorphic with respect to the complex structure J_k . In addition, if this complex structure does not depend on k , as described by Eq. (6), all λ_k are meromorphic functions of the same complex variable $Z = X + iY$, which is only unique

up to global conformal transformation. In particular, rotation and rescaling allows one to set the image of $Z(a_1) = 1$ and $Z(a_2) = \tau$ for a certain complex parameter τ . The existence of a common complex variable Z for all λ_k allows for analytical progress since pseudoperiodic meromorphic functions on the torus are entirely determined by their boundary conditions and by the position of their zeros and poles.

To study these zeros and poles, we fix k and introduce the auxiliary function $\mu_k = \partial_Z \ln \lambda_k = (\partial_Z \lambda_k) / \lambda_k$. It has simple poles with residue equal to 1 and -1 for each of the \mathcal{N}_z zeros and \mathcal{N}_p poles of λ_k , respectively. The contour integral of μ_k over the unit cell is thus equal to the difference $\mathcal{N}_z - \mathcal{N}_p$. On the other hand, the periodicity of μ_k requires this integral to vanish. Therefore, λ_k has as many poles as it has zeros, $\mathcal{N}_z = \mathcal{N}_p = \mathcal{N}$. We respectively denote them as Z_0^j and Z_k^j with $j = 1 \dots \mathcal{N}$. These poles and zeros fully specify the functional form of the meromorphic functions

$$\lambda_k(r) = C_k e^{i\alpha_k Z} \prod_{j=1}^{\mathcal{N}} \frac{\theta_1(Z - Z_k^j; \tau)}{\theta_1(Z - Z_0^j; \tau)}, \quad (7)$$

up to a constant C_k . The boundary conditions $\lambda_k(r + a_j) = e^{ik_j} \lambda_k(r)$ specify the real parameter α_k through [48]

$$e^{ik_1} = e^{i\alpha_k}, \quad e^{ik_2} = e^{i\tau\alpha_k + 2i\pi\mathcal{N}(S_k - S_0)}, \quad S_k = \frac{\sum_j Z_k^j}{\mathcal{N}}. \quad (8)$$

Assuming the Bloch eigenvectors to have no singularities for physical groundedness, the Z_k 's are a subset of the ψ_k 's zeros for each k . We dub them “moving” zeros as they change when k is varied. Equation (8) describes the motion of the center of mass of these moving zeros as k moves in the Brillouin zone. This motion is precisely that of the zero of LLL wavefunction on a torus [42]. We now consider different cases depending on the value of \mathcal{N} .

A direct consequence of our criterion, Eq. (6), is that there must be at least one moving zero $\mathcal{N} \geq 1$. Indeed, $\mathcal{N} = 0$ produces a constant $\alpha_k = 0$ that cannot satisfy the condition imposed by Eq. (8). We then focus on the important case of a single moving zero $\mathcal{N} = 1$. There, $Z_k = \alpha_k$ matches the position of the zero in a LLL on the torus. We realize that the ratio $\phi_k(X, Y) / \phi_0(X, Y)$ possesses the same boundary condition, the same zeros, and the same poles as λ_k . Both functions being meromorphic in $Z = X + iY$, they must be equal up to a constant. In other words, states of the bands can be written as

$$\psi_k(r) \equiv \frac{e^{-\tilde{\rho}(r)}}{N_k} \phi_k(X, Y), \quad e^{-\tilde{\rho}(r)} = \left| \frac{\psi_0(r)}{\phi_0(X, Y)} \right|, \quad (9)$$

where the phase of the ratio $\psi_0(r) / \phi_0(X, Y)$ does not change the overlaps nor the phase factors in the analog LLL, and can thus be absorbed into the boundary condition sewing function s . This brings us back to the case treated above for r -ideal bands, and hence completes the proof.

We have shown that our criterion, Eq. (6), applied in a band with a single moving zero and where $\psi_0(r)$ only vanishes polynomially, implies LLL mapping in its most general form. We note that the two additional assumptions on the number of moving zeros and the absence of essential singularity are satisfied for $|C| = 1$ bands obtained at all magic angles of the chiral model for twisted bilayer graphene [49].

More than one zero. Turning to a situation with more than one zero reveals a novel phenomenology of holomorphic bands. To see this, consider a single band satisfying Eq. (6) and featuring $\mathcal{N} > 1$ moving zeros. This band can only be identified as a strict subset of a $\mathcal{L}(g, B)$ with $N_\phi = \mathcal{N}$ flux per unit cell, the exact mapping between the two systems being proscribed by the larger N_ϕ -fold degeneracy of LLL at each k point [42]. While it is not clear whether this situation is compatible with a spectral gap isolating the band in energy, we were not able to rule it out. The properties of such a band would be determined by the specific cut it defines within the larger $\mathcal{L}(g, B)$ manifold, and cannot be solely inferred from the properties of the LLL. That is, holomorphic bands with $\mathcal{N} > 1$ should go beyond the physics of a LLL.

From a different perspective, we see that such bands are incompatible with the r -idealness condition—they are not stable under multiplication by Z . Should they be, the system would necessarily exhibit an \mathcal{N} -fold degeneracy at each point of the Brillouin zone, and precisely map onto an LLL featuring the same number of moving zeros [42]. This again highlights that r -idealness is equivalent to LLLs, even in the case of multiple bands.

Greater Chern numbers. Let us finally comment on the case of a band with Chern number $|C| > 1$. Early in the study of Chern bands, it was shown that such bands could be described as $|C|$ bands distinguished by a “color” index upon extending the unit cell $|C|$ times, where all the colored bands carry a Chern number $\text{sign}(C)$ and are intertwined through real-space translations by $a_{1/2}$, the original Bravais lattice vectors [50,51]. When these colored bands took the form of “flat ideal bands” with Chern number $C_\sigma = 1$, i.e., of Landau levels with uniform magnetic field and metric, this construction provided flat ideal bands with larger Chern $|C| > 1$ dubbed color entangled [35]. More recently, q -ideal bands with $|C| > 1$ were also written as color-entangled bands where each of the colored bands with unit Chern number was itself a q -ideal band [52,53], i.e., they mapped to Landau levels with spatially varying magnetic field but uniform metric.

One of the main ideas of the present work is that the most generic ideal Chern band should ensue from the most generic Landau level, which possess both a nonuniform magnetic field and a nonuniform metric. Similarly, the most generic color-entangled ideal bands should be built from the Landau levels of Eq. (2) including the nonlinear embedding of the unit cell provided by the isothermal coordinates (X, Y) . In the Supplemental Material [42], we prove that applying the criterion, Eq. (6), to the colored bands of a generic band with a Chern number $C > 1$ yields precisely to this generalization. Thus, the framework presented here still applies provided we first disentangle the different “colors” of the band.

Conclusion. In this work, we have shown that all ideal Chern bands introduced in the literature map onto LLLs in curved space. Conversely, equivalence to the most general LLL does not lead to novel ideal bands beyond r -ideal bands. This proves that we have exhausted all possible criteria expressing Chern idealness as some flavor of LLL mapping. We have also designed an operational criterion to identify which bands can be mapped onto the most general periodic LLLs. This criterion solely relies on the inexpensive evaluation of Bloch wavefunctions’ derivatives.

Acknowledgments. We thank J. Wang for useful comments. This work has benefited from discussions held at the 2023 Quantum Geometry Working Group meeting that took place at the Flatiron Institute. The Flatiron Institute is a division

of the Simons Foundation. N.R. acknowledges support from the QuantERA II Programme that has received funding from the European Union's Horizon 2020 research and innovation program under Grant Agreement No. 101017733.

-
- [1] E. Tang, J.-W. Mei, and X.-G. Wen, High-Temperature Fractional Quantum Hall States, *Phys. Rev. Lett.* **106**, 236802 (2011).
- [2] T. Neupert, L. Santos, C. Chamon, and C. Mudry, Fractional Quantum Hall States at Zero Magnetic Field, *Phys. Rev. Lett.* **106**, 236804 (2011).
- [3] D. Sheng, Z.-C. Gu, K. Sun, and L. Sheng, Fractional quantum Hall effect in the absence of Landau levels, *Nat. Commun.* **2**, 389 (2011).
- [4] N. Regnault and B. A. Bernevig, Fractional Chern Insulator, *Phys. Rev. X* **1**, 021014 (2011).
- [5] H. L. Stormer, D. C. Tsui, and A. C. Gossard, The fractional quantum Hall effect, *Rev. Mod. Phys.* **71**, S298 (1999).
- [6] V. Crépel, B. Estienne, B. A. Bernevig, P. Lecheminant, and N. Regnault, Matrix product state description of Halperin states, *Phys. Rev. B* **97**, 165136 (2018).
- [7] T. H. Hansson, M. Hermanns, S. H. Simon, and S. F. Viefers, Quantum Hall physics: Hierarchies and conformal field theory techniques, *Rev. Mod. Phys.* **89**, 025005 (2017).
- [8] V. Crépel, N. Regnault, and B. Estienne, Matrix product state description and gaplessness of the Haldane-Rezayi state, *Phys. Rev. B* **100**, 125128 (2019).
- [9] J. Jain, Theory of the fractional quantum Hall effect, *Phys. Rev. B* **41**, 7653 (1990).
- [10] J. K. Jain, Composite fermion theory of exotic fractional quantum Hall effect, *Annu. Rev. Condens. Matter Phys.* **6**, 39 (2015).
- [11] V. Crépel, N. Claussen, and B. Estienne, Microscopic study of the Halperin–Laughlin interface through matrix product states, *Nat. Commun.* **10**, 1860 (2019).
- [12] G. Moore and N. Read, Nonabelions in the fractional quantum Hall effect, *Nucl. Phys. B* **360**, 362 (1991).
- [13] A. Stern, Anyons and the quantum Hall effect—A pedagogical review, *Ann. Phys.* **323**, 204 (2008).
- [14] V. Crépel, N. Claussen, and B. Estienne, Model states for a class of chiral topological order interfaces, *Nat. Commun.* **10**, 1861 (2019).
- [15] D. J. Clarke, J. Alicea, and K. Shtengel, Exotic non-Abelian anyons from conventional fractional quantum Hall states, *Nat. Commun.* **4**, 1348 (2013).
- [16] V. Crépel, B. Estienne, and N. Regnault, Variational Ansatz for an Abelian to Non-Abelian Topological Phase Transition in $\nu = 1/2 + 1/2$ Bilayers, *Phys. Rev. Lett.* **123**, 126804 (2019).
- [17] D. Arovas, J. R. Schrieffer, and F. Wilczek, Fractional Statistics and the Quantum Hall Effect, *Phys. Rev. Lett.* **53**, 722 (1984).
- [18] S. H. Simon, The Chern–Simons Fermi liquid description of fractional quantum Hall states, *Composite Fermions: A Unified View of the Quantum Hall Regime* (World Scientific, Singapore, 1998), pp. 91–194.
- [19] V. Crépel, B. Estienne, and N. Regnault, Microscopic study of the coupled-wire construction and plausible realization in spin-dependent optical lattices, *Phys. Rev. B* **101**, 235158 (2020).
- [20] R. Roy, Band geometry of fractional topological insulators, *Phys. Rev. B* **90**, 165139 (2014).
- [21] G. Tarnopolsky, A. J. Kruchkov, and A. Vishwanath, Origin of Magic Angles in Twisted Bilayer Graphene, *Phys. Rev. Lett.* **122**, 106405 (2019).
- [22] O. Vafek and J. Kang, Renormalization Group Study of Hidden Symmetry in Twisted Bilayer Graphene with Coulomb Interactions, *Phys. Rev. Lett.* **125**, 257602 (2020).
- [23] N. Bultinck, E. Khalaf, S. Liu, S. Chatterjee, A. Vishwanath, and M. P. Zaletel, Ground State and Hidden Symmetry of Magic-Angle Graphene at Even Integer Filling, *Phys. Rev. X* **10**, 031034 (2020).
- [24] B. Lian, Z.-D. Song, N. Regnault, D. K. Efetov, A. Yazdani, and B. A. Bernevig, Twisted bilayer graphene. IV. Exact insulator ground states and phase diagram, *Phys. Rev. B* **103**, 205414 (2021).
- [25] B. A. Bernevig, B. Lian, A. Cowsik, F. Xie, N. Regnault, and Z.-D. Song, Twisted bilayer graphene. V. Exact analytic many-body excitations in Coulomb Hamiltonians: Charge gap, goldstone modes, and absence of cooper pairing, *Phys. Rev. B* **103**, 205415 (2021).
- [26] V. Crépel, A. Dunbrack, D. Guerci, J. Bonini, and J. Cano, Chiral model of twisted bilayer graphene realized in a monolayer, *Phys. Rev. B* **108**, 075126 (2023).
- [27] V. Crépel and L. Fu, Anomalous Hall metal and fractional Chern insulator in twisted transition metal dichalcogenides, *Phys. Rev. B* **107**, L201109 (2023).
- [28] V. Crépel, N. Regnault, and R. Queiroz, The chiral limits of moiré semiconductors: Origin of flat bands and topology in twisted transition metal dichalcogenides homobilayers, [arXiv:2305.10477](https://arxiv.org/abs/2305.10477).
- [29] M. Claassen, C. H. Lee, R. Thomale, X.-L. Qi, and T. P. Devereaux, Position-Momentum Duality and Fractional Quantum Hall Effect in Chern Insulators, *Phys. Rev. Lett.* **114**, 236802 (2015).
- [30] B. Mera and T. Ozawa, Engineering geometrically flat Chern bands with Fubini-study Kähler structure, *Phys. Rev. B* **104**, 115160 (2021).
- [31] B. Mera and T. Ozawa, Uniqueness of Landau levels and their analogs with higher Chern numbers, [arXiv:2304.00866](https://arxiv.org/abs/2304.00866).
- [32] J. Wang, J. Cano, A. J. Millis, Z. Liu, and B. Yang, Exact Landau Level Description of Geometry and Interaction in a Flatband, *Phys. Rev. Lett.* **127**, 246403 (2021).
- [33] P. J. Ledwith, A. Vishwanath, and D. E. Parker, Vortexability: A unifying criterion for ideal fractional Chern insulators, [arXiv:2209.15023](https://arxiv.org/abs/2209.15023).
- [34] F. D. M. Haldane, Fractional Quantization of the Hall Effect: A Hierarchy of Incompressible Quantum Fluid States, *Phys. Rev. Lett.* **51**, 605 (1983).
- [35] Y.-L. Wu, N. Regnault, and B. A. Bernevig, Haldane statistics for fractional Chern insulators with an arbitrary Chern number, *Phys. Rev. B* **89**, 155113 (2014).

- [36] R. Alicki, J. R. Klauder, and J. Lewandowski, Landau-level ground-state degeneracy and its relevance for a general quantization procedure, *Phys. Rev. A* **48**, 2538 (1993).
- [37] S. Klevtsov, Random normal matrices, Bergman kernel and projective embeddings, *J. High Energy Phys.* **01** (2014) 133.
- [38] S. Klevtsov, Geometry and large n limits in Laughlin states, [arXiv:1608.02928](https://arxiv.org/abs/1608.02928).
- [39] S. Klevtsov, Lowest Landau level on a cone and zeta determinants, *J. Phys. A: Math. Theor.* **50**, 234003 (2017).
- [40] B. A. Dubrovin and S. P. Novikov, Ground states of a two-dimensional electron in a periodic magnetic field, *Sov. Phys. JETP* **52**, 511 (1980).
- [41] C. F. Gauss, Allgemeine Auflösung der Aufgabe die Theile einer gegebenen Fläche auf einer andern gegebenen Fläche so abzubilden dass die Abbildung dem Abgebildeten in den kleinsten Theilen ähnlich wird, *Gauss Werke Band 4*, 189 (1825).
- [42] See Supplemental Material at <http://link.aps.org/supplemental/10.1103/PhysRevResearch.5.L032048> for additional details on isothermal coordinates, the form of LLL function on the torus, application of our criterion to known ideal bands and generalization to $|C| > 1$, which contains Refs. [8,28,32,33,35,43,46–48,50–53].
- [43] J. Dong, J. Wang, and L. Fu, Dirac electron under periodic magnetic field: Platform for fractional Chern insulator and generalized Wigner crystal, [arXiv:2208.10516](https://arxiv.org/abs/2208.10516).
- [44] B. Mera and T. Ozawa, Kähler geometry and Chern insulators: Relations between topology and the quantum metric, *Phys. Rev. B* **104**, 045104 (2021).
- [45] We can always choose a positive since only $|e^{-\tilde{\rho}}|$ appears in the overlaps and form factors of the Chern band [32]. Any additional phase can be absorbed in the boundary condition sewing function s .
- [46] M. R. Douglas and S. Klevtsov, Bergman kernel from path integral, *Commun. Math. Phys.* **293**, 205 (2010).
- [47] G. Konstantinou and K. Mouloupoulos, The “forgotten” pseudomomenta and gauge changes in generalized Landau level problems: Spatially nonuniform magnetic and temporally varying electric fields, *Int. J. Theor. Phys.* **56**, 1484 (2017).
- [48] DLMF, NIST Digital Library of Mathematical Functions, edited by F. W. J. Olver, A. B. Olde Daalhuis, D. W. Lozier, B. I. Schneider, R. F. Boisvert, C. W. Clark, B. R. Miller, B. V. Saunders, H. S. Cohl, and M. A. McClain, <https://dlmf.nist.gov/>, release 1.1.9 of 2023-03-15.
- [49] J. Wang, Y. Zheng, A. J. Millis, and J. Cano, Chiral approximation to twisted bilayer graphene: Exact intravalley inversion symmetry, nodal structure, and implications for higher magic angles, *Phys. Rev. Res.* **3**, 023155 (2021).
- [50] M. Barkeshli and X.-L. Qi, Topological Nematic States and Non-Abelian Lattice Dislocations, *Phys. Rev. X* **2**, 031013 (2012).
- [51] Y.-L. Wu, N. Regnault, and B. A. Bernevig, Gauge-fixed Wannier wave functions for fractional topological insulators, *Phys. Rev. B* **86**, 085129 (2012).
- [52] J. Wang, S. Klevtsov, and Z. Liu, Origin of model fractional Chern insulators in all topological ideal flatbands: Explicit color-entangled wavefunction and exact density algebra, *Phys. Rev. Res.* **5**, 023167 (2023).
- [53] J. Dong, P. J. Ledwith, E. Khalaf, J. Y. Lee, and A. Vishwanath, Exact many-body ground states from decomposition of ideal higher Chern bands: Applications to chirally twisted graphene multilayers, *Phys. Rev. Res.* **5**, 023166 (2023).